A Molecular Orbital Study of the Role of BH_5 in the Hydrolysis of BH_4^-

Irene M. Pepperberg, Thomas A. Halgren, and William N. Lipscomb*[1]

Contribution from the Gibbs Chemical Laboratory, Harvard University, Cambridge, Massachusetts 02138. *Received October 20, 1975*

Abstract: Molecular orbital methods are employed to examine the structure and stability of BH_5 in the light of results for aqueous hydrolysis of BH_4^-. These results suggest that BH_5 exists as a metastable intermediate. The optimal BH_5 geometry for a given constraint in B–H distance is found to have C_s symmetry, and to have identifiable BH_3 and H_2 subunits consistent with the experimental expectations for the intermediate in hydrolysis. However, single determinant calculations using PRDDO and STO-3G minimum basis sets and 4-31G and double ζ plus polarization extended basis sets indicate that BH_5 is unstable with respect to dissociation to BH_3 and H_2 by ≥ 10 kcal/mol. The stabilization of BH_5 relative to BH_3 and H_2 from configuration interaction is estimated to be ≈ 10 kcal/mol. Studies of solvation effects using specific hydration and statistical interaction models indicate that the product BH_3 is stabilized in solution by ~ 6 kcal/mol by formation of a $H_2O{:}BH_3$ complex. Representative BH_5 structures are stabilized by much smaller amounts of 2–3 kcal/mol. The net result is that the experimental and computational results cannot now be reconciled within limits of a few kilocalories per mole, presumably because of limitations in the theoretical procedures. Less sensitive aspects of the chemistry of BH_5 are examined using PRDDO, and in some cases 4-31G, calculations. These aspects include (a) a study of electronically allowed and disallowed dissociations from BH_5 of molecular hydrogen by means of various hydrogen atom pairings in each of the D_{3h}, C_{4v}, and C_{2v} structures, (b) a comparison of bonding interactions in BH_5 and CH_5^+ using localized molecular orbital techniques, and (c) a consideration of pathways for intramolecular rearrangement in C_s structures for BH_5.

The pentacoordinated boranes BH_5 and BH_4D have been proposed[2-6] as intermediates in the hydrolysis and deuterolysis of borohydride ion, BH_4^-. The role of these borane intermediates appears to be similar to that proposed for the isoelectronic CH_5^+ in the protonation of CH_4 by strong acids; furthermore, the frequent use of boranes (BH_3, R_3B) as models for the carbenium ions (CH_3^+, R_3C^+)[7,8] might suggest analogous properties for BH_5 and CH_5^+.

As a chemical species, CH_5^+ has been well characterized, both experimentally in gas phase[9] and solution studies,[10] and theoretically, through molecular orbital calculations employing a variety of levels of sophistication.[11-19] By all accounts, the most stable form displays C_s symmetry and has two relatively long and three normal C–H bond lengths. Although readily recognizable as a complex between CH_3^+ and H_2,[12] this form is stable with respect to dissociation either to CH_3^+ and H_2[15,18,19] or to CH_4 and H^+.[18]

As noted above, one might expect the less extensively studied BH_5 to have properties analogous to those of CH_5^+. However, a neutral BH_3 should be much less attractive than CH_3^+ as a coordination site for H_2. Furthermore, BH_3 has an empty valence orbital, but H_2 does not, and hence the crucial reciprocal donor–acceptor role played, for example, by each BH_3 subunit in B_2H_6[20,21] would not be applicable here. In CNDO/2 calculations by Olah et al., BH_5 was found to have C_s symmetry similar to that of CH_5^+. Although the CNDO/2 studies were performed primarily to determine the preferred geometry for BH_5, the calculations also predicted a binding energy for BH_5 of 960 kcal/mol.[5] A more accurate calculation might establish that only a marginally stable structure exists for BH_5.

Nevertheless, experimental studies[2-6] on the reactions of BH_4^- (or BD_4^-) in D_2O and H_2O at varying pH appear strongly to support the existence of a pentacoordinated (BH_5, BH_4D, etc.) intermediate which can: (a) lose a proton to form BH_3D^- (exchange); (b) lose molecular hydrogen to form BH_3 and HD (hydrolysis); or (c) first undergo an internal rearrangement (scrambling) which ultimately makes possible the formation of BH_2D and H_2 (Figure 1). Thus, in D_2O, BH_4^- can evolve hydrogen and/or take up deuterium from the solvent to form, successively, BH_3D^-, $BH_2D_2^-$, etc. At pD ≤ 12, the protonation of BH_4^- (shown schematically in Figure 1) is mainly effected by D_3O^+.[4] Here, the relative ratio for hydrogen loss (mainly HD) and deuterium exchange is essentially constant ($\sim 1{:}10$)[22] because the concentration of D_2O, the predominant base for abstraction of H^+ or D^+, is itself constant ($[D_2O] \simeq 55$ M). The total rate is then proportional to the D_3O^+ concentration, and the rate of scrambling is extremely small.[3] Above pD 12, the total rate becomes essentially constant, reflecting protonation by D_2O, but deuterium exchange increasingly predominates over hydrolysis as the OD^- concentration rises above ~ 0.1 M; at pD > 14, only the exchange with solvent is evident.[23] The proposed intermediate thus appears to be BH_5 (or BH_4D, etc.), and might indeed be written as $BH_3{:}HD$ to account for the fact that nearly all of the hydrogen evolved in the deuterolysis of BH_4^- is HD.[2-4,6]

Olah and co-workers have observed an essentially statistical composition of evolved molecular hydrogen for the reaction of, e.g., solid $NaBH_4$ with anhydrous D_2SO_4 or DF.[5] However, because of several factors associated with the rather different conditions employed in these experiments, we shall focus primarily on the better characterized results in aqueous solution.

Despite difficulties inherent in modeling a process which occurs in solution, BH_5 is an attractive system for a molecular orbital study. Its small size would leave room for an appreciable elaboration of the computational model itself, if necessary, in order to reconcile the theoretical predictions with the experimental results. Somewhat to our surprise, we have found such a reconciliation extremely difficult to effect. The difficulty probably arises from limitations in the computational models selected, and/or from limitations in the procedures available to us for taking the aqueous environment into account. We offer this study, in part, as an object lesson in the application of present quantum mechanical techniques to a difficult problem, which should be useful for the development and refinement of improved computational models. In addition, we investigate several aspects of the behavior of BH_5 which we believe can properly be chronicled by our relatively simple physical model.

We shall first report calculations for several nuclear configurations for BH_5 which are based on those proposed[9-19] for the isoelectronic CH_5^+. For the most part, these calculations have been carried out in the approximation of partial retention of diatomic differential overlap (PRDDO),[24] a rapid, nonempirical SCF method which has afforded results of es-

sentially ab initio minimum basis set quality.[20,24,25] We employ molecular energies, molecular orbitals localized by the method of Boys[26,27] (LMO's), overlap populations, atomic charges, and electron density maps[28] to compare the bonding in BH_5 and CH_5^+. Principal results are explicitly tested with the use of minimal STO-3G and extended 4-31G calculations[29] and by a further extension of the basis set to double ζ plus polarization functions.[30] The effects of a limited inclusion of configuration interaction[31] on the dissociation of BH_5 to BH_3 and H_2 are also considered. In addition, both statistical interaction and specific hydration models are employed in order to examine the effects of solvation on the energy of BH_5 relative to $BH_3 + H_2$.

Preceding these results we conduct a geometry search for BH_5, study the electronically allowed and disallowed processes for loss of various pairs of H atoms from BH_5, and investigate, using PRDDO and 4-31G theoretical methods, the pathways for internal rearrangements in BH_5.

Minimum Basis Set Results

Geometry Search for BH_5. Minimum basis set PRDDO calculations using the exponents listed in Table I gave rise to the structures shown in Figures 2a–d (Table II). With the exception of the C_s structure shown in Figure 2d, each was fully optimized within the symmetry imposed (D_{3h}, C_{4v}, C_{2v}). Symmetry restrictions were then successively removed, and all bond angles and internuclear distances were sequentially refined until consecutive full cycles yielded structures which differed by less than 1.0° in bond angles and 0.01 au in internuclear distances, or until dissociation to BH_3 and H_2 was clearly indicated. No structure for BH_5 was found to be stable with respect to dissociation to BH_3 and H_2 at the PRDDO level. The details of the calculations upon removal of the symmetry restrictions are as follows.

D_{3h}. Starting from the optimized D_{3h} structure shown in Figure 2a, an initial angular refinement of the axial hydrogens resulted in a monotonic decrease in energy and led to either the C_{4v} structure (Figure 3a) or a C_{2v} structure (Figure 3b). The final structure obtained depended on the direction of the initial variation.

C_{4v}. Continuous displacements of the atoms from the optimized C_{4v} geometry (Figure 2b) toward either C_{2v} (Figure 3c) or C_s symmetry positions (Figure 3c′) via linear synchronous transit pathways[32] were accompanied by monotonic decreases in energy. As Figure 3c indicates, the pathway to C_{2v} symmetry consists primarily of a rotation of H2, H3, and H4 about the central boron atom, while the deformation to C_s symmetry involves mainly the motion of H4 and H5.

C_{2v}. Removal of the constraint of C_{2v} symmetry resulted in the migration of H4 toward H5 (or H1) (Figure 3d) and in rapid increases in the B–H4 and B–H5 (or B–H1) distances. The remaining atoms progressively assumed the planar geometry characteristic of BH_3, and the result was dissociation to BH_3 and H_2 (Figure 3f).

C_s. In this case, C_s symmetry was maintained (Figure 2d), but the hydrogen–boron lengths, which previously had been fixed at 2.28 au for the C_s structure, were fully optimized. This refinement resulted in rapid increases in the B–H4 and B–H5 distances. Further, the B–H1, B–H2, and B–H3 bond lengths shortened until they corresponded to those of BH_3; we again observed dissociation to BH_3 and H_2 (Figure 3e). Particular structures along this dissociation curve (Figure 4) are further discussed below. The structure having common B–H bond lengths of 2.28 au will be called C_s(I), while those having distal B–$H_{4,5}$ lengths of 2.55 and 2.81 au will be denoted, respectively, as C_s(II) and C_s(III).

Pathways for Expulsion of H_2. Given that all the PRDDO structures for BH_5 are less stable than $BH_3 + H_2$ (Table III), it might at first appear that the molecule of hydrogen evolved could readily form from any of the ten pairs [5 × ½] of hydrogen atoms in BH_5. This, however, is not the case. We find instead that H_2 must ultimately be derived from one axial and

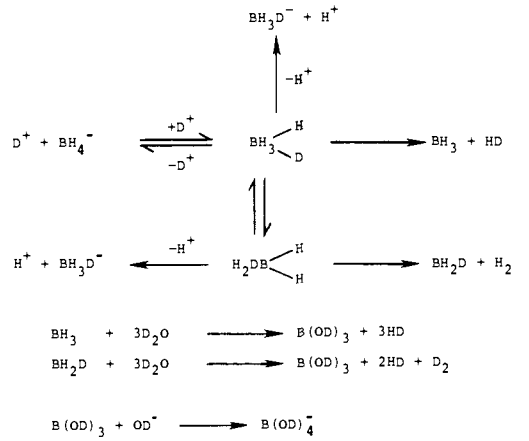

Figure 1. A schematic mechanism for reaction of BH_4^- in D_2O.

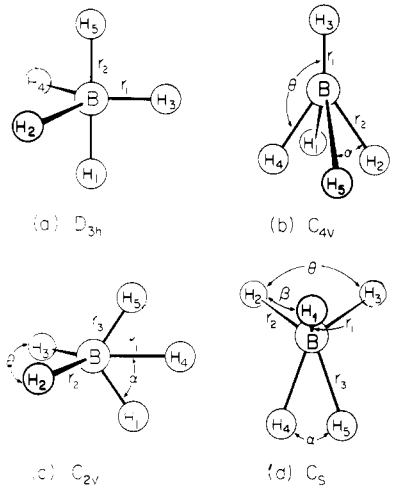

Figure 2. Possible structures for BH_5. (a) D_{3h}: threefold axis linear with H_1–B–H_5, r_1 = 2.252 au, r_2 = 2.280 au. (b) C_{4v}: fourfold axis along H_3–B; r_1 = 2.172 au, r_2 = 2.287 au, θ = 117.3°, α = 77.9°. (c) C_{2v}: twofold axis collinear with H_4–B, r_1 = 2.492 au, r_2 = 2.191 au, r_3 = 2.370 au, θ = 123.0°, α = 56.0°. (d) C_s: symmetry plane bisects ∠H_4–B–H_5. C_s(I): $r_1 = r_2 = r_3$ = 2.280 au, θ = 106.8°, α = 46.6°, β = 116.4°. C_s(II): r_1 = 2.182 au, r_2 = 2.225 au, r_3 = 2.555 au, θ = 108.8°, α = 38.0°, β = 117.1°. C_s(III): r_1 = 2.192 au, r_2 = 2.205 au, r_3 = 2.807 au, θ = 115.4°, α = 32.1°, β = 117.4°.

Table I. Exponents

		Minimum basis set				
BH_5	B	1s	4.6838	H^a	1s	1.136
		2s	1.4489	H^b	1s	1.2
		2p	1.4836			
CH_5^{+c}	C	1s	5.68	H1	1s	1.26
		2s	1.75	H4	1s	1.29
		2p	1.75			
CH_3^{+c}	C	1s	5.68	H	1s	1.31
		2s	1.75			
		2p	1.75			
H_2				H	1s	1.2

[a] Exponents are for all normal and distal hydrogens for all structures, including BH_3, but excluding the distal hydrogens in the C_s(V) structure (distal B–H distance of 6.2 au). [b] This is the exponent for the distal hydrogens which form the H_2 subunit in the C_s(V) structure. [c] Reference 14.

Table II. Coordinates[a]

			x	y	z
BH_5	D_{3h}	B	0.0	0.0	0.0
		H2	−1.125 5	1.949 42	0.0
		H3	2.251	0.0	0.0
		H5	0.0	0.0	2.280
	C_{4v}	B	0.0	0.0	0.0
		H1	1.437 49	1.437 49	−1.047 67
		H3	0.0	0.0	2.171 996
	C_{2v}	B	0.0	0.0	0.0
		H1	1.325 24	0.0	1.964 84
		H2	−1.045 47	1.925 47	0.0
		H4	2.492	0.0	0.0
	C_s[b](I)	B	0.0	0.0	0.0
		H1	0.0	1.765 37	−1.144 63
		H2	1.826 06	−0.211 01	1.340 43
		H4	0.904 27	−1.805 03	−1.074 45
	C_s[c](II)	B	0.0	0.0	0.0
		H1	0.0	1.638 59	−1.440 88
		H2	1.808 51	−0.225 67	1.275 85
		H4	0.831 31	−2.095 86	−1.201 31
	C_s[d](III)	B	0.0	0.0	0.0
		H1	0.0	1.541 12	1.558 78
		H2	1.864 25	−0.287 18	−1.142 00
		H4	0.776 25	−2.266 53	1.462 72
CH_5^+	C_s	C	0.0	0.0	0.0
		H1	1.961 63	0.0	−0.530 74
		H2	−0.980 84	1.698 79	−0.530 74
		H4	0.0	0.849 69	2.388 51
CH_3^+	D_{3h}	C	0.0	0.0	0.0
		H1	2.045 23	0.0	0.0
		H2	−1.022 67	−1.771 19	0.0
H_2		H1	0.7	0.0	0.0

[a] Coordinates are given in atomic units. [b] Distal B–H lengths are 2.29 au. [c] Distal B–H lengths are 2.56 au. [d] Distal B–H lengths are 2.81 au.

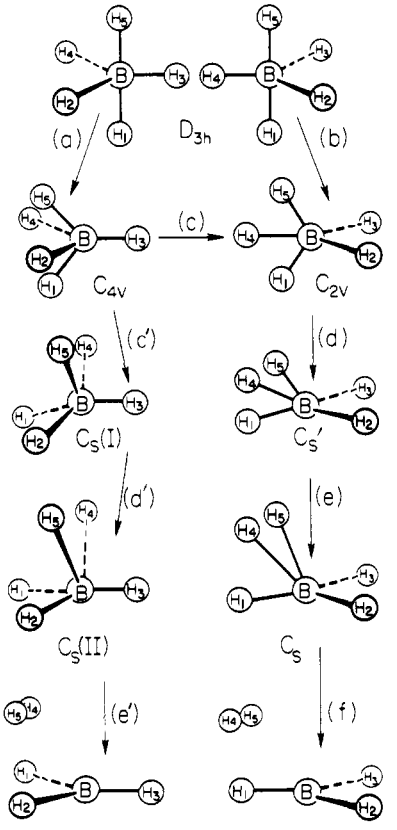

Figure 3. Structures obtained by successive removal of symmetry restrictions for BH_5.

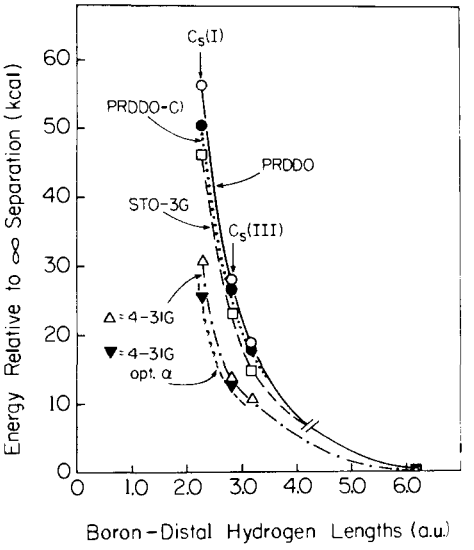

Figure 4. Variation of energy as a function of distal hydrogen–boron distances (C_s pathway) for BH_5, with respect to $BH_3 + H_2$ at infinite separation. For the minimum basis set calculations, the exponents on the distal hydrogens were changed from 1.136 to 1.2 at the break in the curve.

one equatorial position of the prototype D_{3h} structure if the evolution of hydrogen is to be spontaneous. For the D_{3h} structure itself, the origin of this preference is evident both in the LMO results (Table IV) and in the atomic overlap populations (Table V). Thus the six D_{3h} axial–equatorial pairs have positive overlap populations of 0.041 e^-, but negative overlap populations are found for the axial–axial (−0.053 e^-) and the

Table III. Energetics[a]

		E(PRDDO)	E_{diss} (PRDDO)	E(PRDDO-CI)	E_{diss}(PRDDO-CI)	E(STO-3G)	E_{diss} (STO-3G)	E(4-31G)	E_{diss} (4-31G)	E(ext-basis)[b,]	E_{diss}(ext. basis)[b]
BH_5	D_{3h}	−27.383				−27.094		−27.386			
	C_{4v}	−27.400				−27.112		−27.403			
	C_{2v}	−27.418				−27.129		−27.423			
	C_s(I)[c]	−27.410	−56.5	−27.478	−50.8	−27.121	−46.4	−27.427	−30.8		
								−27.435[d]			
	C_s(II)	−27.438									
	C_s(III)	−27.456	−28.5	−27.516	−27.0	−27.158	−23.2	−27.454	−13.8	−27.516[e]	−9.7[e]
								−27.457[d]	−12.0	−27.519[f]	−10.0[f]
	C_s(IV)	−27.471	−18.8	−27.530	−18.2	−27.171	−15.1	−27.459	−10.7		
	C_s(V)	−27.500[g]	−0.6			−27.194[g]	−0.6	−27.475	−0.6		
BH_3 + $H_2(\infty)$		−27.501		−27.559		−27.195		−27.476		−27.532[e]	
										−27.535[f]	
H_2		−1.129		−1.147		−1.119		−1.127		−1.130[e]	
										−1.134[f]	
CH_5^+	C_s	−40.311	2.6	−40.394	8.7	−39.915[h]		−40.322[i]			
						−39.919[i]	13.7[i]	−40.327[j]	15.8		
CH_3^+	D_{3h}	−39.178		−39.233		−38.780[i]		−39.175[i]			
CH_3^+ + H_2		−40.307		−40.380		−39.897[i]		−40.302[i]			
BH_4^-		−26.965				−26.634		−26.923			

[a] Energies are in atomic units (1 au = 627.57 kcal); E_{diss} is in kcal/mol. [b] Ext. basis refers to calculations employing a double ζ plus polarization extended basis set. [c] Each C_s structure represents different distal B-H bond lengths: (I) represents 2.287 au, (II) represents 2.555 au; (III) represents 2.807 au; (IV) represents 3.167 au; (V) represents 6.204 au. [d] Distal H-B-H angle has been optimized in these calculations. [e] The LSL basis set (cf. ref 21) was used in these calculations. This includes the H_2 calculation for BH_3 + H_2. The energy difference when the FR basis is used for H_2 is 11.9 kcal/mol. [f] The FR basis set (cf. ref 39) was used for the H_2 subunit in these calculations. [g] Calculations were performed with hydrogen exponents for the distal hydrogens. [h] This calculation employs the exponents of Mulder and Wright (cf. ref 14). [i] Reference 16. [j] Reference 19.

Table IV. Localized Orbitals

Structure		LMO A-B-C	Populations[a] A	B	C	% delocalization[b]
BH_5	D_{3h}	B(1)[c]	2.01			4.1
		B-H5 (1)	0.83	0.85		19.5
		B-H3-H1 (3)	0.81	0.97	0.22	13.9
	C_{4v}	B (1)	2.01			4.0
		B-H2 (1)	0.77	0.96		18.1
		B-H3 (1)	0.89	1.13		7.3
		B-H1-H4 (1)	0.77	0.78	0.45	17.3
		B-H5-H4 (1)	0.77	0.81	0.41	17.3
	C_{2v}[d]	B (1)	2.01			3.6
		B-H2 (2)	0.89	1.12		10.5
		B-H4-H5 (2)	0.62	0.39	1.01	15.2
	C_{2v}*[e]	B (1)	2.01			3.0
		B-H3 (1)	0.86	1.08		11.3
		B-H1-H5 (1)	0.57	0.97	0.38	10.1
		B-H2-H5 (1)	0.78	0.95	0.27	10.9
		B-H4-H5 (1)	0.76	0.93	0.31	11.0
	C_s(II)[f]	B (1)	2.01			3.5
		B-H1 (1)	0.89	1.14		9.3
		B-H2 (2)	0.87	1.11		10.9
		B-H4-H5 (1)	0.32	0.86	0.86	10.1
	C_s(III)[g]	B (1)	2.01			3.3
		B-H1 (1)	0.89	1.14		9.6
		B-H2 (2)	0.89	1.13		10.0
		B-H4-H5 (1)	0.21	0.91	0.91	9.0
CH_5^+	C_s	C (1)	2.00			2.5
		C-H1 (1)	0.83	1.19		9.5
		C-H2 (2)	0.82	1.18		9.8
		C-H4-H5 (1)	0.58	0.72	0.72	8.7

[a] These values are reported in order of atoms listed under LMO. [b] The delocalization is $[\frac{1}{2}\int(\phi - \phi^T)^2\, d\tau]^{1/2}$ where ϕ is an LMO and ϕ^T is obtained from ϕ by truncating nonlocal contributions and renormalizing, cf. ref 26. [c] The number in parentheses is the number of bonds of this type or the number of inner shells. [d] This original optimized structure of C_{2v} symmetry is also obtained by concerted swing of H2-H4 (or H1-H5) starting from the C_{4v} configuration. [e] This structure is obtained from the motion needed to expel H1 and H5 directly from the C_{4v} configuration. [f] This structure is along the BH_5 dissociation pathway of C_s symmetry; it has B-H distal lengths of 2.55 au. [g] This structure, also along the dissociation pathway of C_s symmetry, has B-H distal lengths of 2.81 au.

Table V. Overlap Populations

	Structures						
	CH_5^+	BH_5					
Pair	C_s	C_s(II)	C_s(III)	D_{3h}	C_{4v}	C_{2v}[a]	C_{2v}*[b]
B(C)-H1	0.77	0.84	0.83	0.67	0.58	0.51	0.66
B(C)-H2	0.75	0.79	0.81	0.59	0.58	0.82	0.66
B(C)-H3	0.75	0.79	0.81	0.67	0.83	0.82	0.29
B(C)-H4	0.27	0.20	0.11	0.59	0.58	0.31	0.77
B(C)-H5	0.27	0.20	0.11	0.67	0.58	0.51	0.29
H1-H2	−0.02	−0.03	−0.03	0.04	0.08	−0.01	−0.05
H1-H3	−0.02	−0.03	−0.03	0.04	−0.03	−0.01	0.05
H1-H4	−0.02	−0.03	−0.03	0.04	0.08	0.21	−0.01
H1-H5	−0.02	−0.03	−0.03	−0.05	−0.09	−0.12	−0.32
H2-H3	−0.02	−0.02	−0.03	−0.07	−0.03	−0.03	0.05
H2-H4	−0.03	−0.00	−0.01	−0.07	−0.09	−0.05	−0.01
H2-H5	−0.01	−0.07	−0.05	0.04	0.08	−0.01	0.05
H3-H4	−0.01	−0.07	−0.05	−0.07	−0.03	−0.05	−0.01
H3-H5	−0.03	0.00	−0.01	0.04	−0.03	−0.01	−0.32
H4-H5	0.41	0.56	0.68	0.04	0.08	0.21	−0.01

[a] This is the original C_{2v} structure which is also obtained by movement of H2, H3, H4 in the C_{4v} configuration (cf. Figure 3c). [b] This is the structure of C_{2v} symmetry obtained by attempting the direct abstraction of H1 and H5 from the C_{4v} configuration.

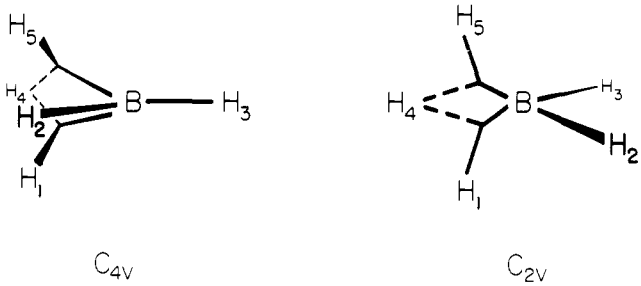

Figure 5. Boys localized orbital representations of the C_{4v} and C_{2v} structures. Solid lines (—) represent contributions from atoms of ≥0.5 e⁻, and dashed lines (- - -) represent contributions of between 0.35 and 0.5 e⁻.

equatorial-equatorial pairs (−0.067 e⁻). The LMO picture reveals that each axial-equatorial pair can take part in one of the three-center H-B-H bonds, one of which can, in turn, smoothly evolve into the molecular orbital of the product hydrogen molecule. Similarly, these axial-equatorial pairs can give rise to the three-center H-B-H bonds present in either the C_{4v} or C_{2v} structures pictured in Figure 5. As might be expected on geometrical grounds, such deformations enhance certain of the three-center interactions at the expense of others, but the overall result is to maintain, to a considerable extent, the original LMO framework. Thus, the four resultant pairs of *neighboring* hydrogens around the square base in the C_{4v} structure have positive overlap populations of 0.075 e⁻. There is a degree of arbitrariness in the molecular orbital localization, since only three MO's are shared around the square base,[33] but this arbitrariness is just sufficient to ensure that any pair of adjacent (axial-equatorial) hydrogens can contribute to a three-center H-B-H bond orbital. We find that any such pair can spontaneously depart as H_2. In contrast, in the C_{4v} structure, interactions involving the formerly axial-axial or equatorial-equatorial pairs H1-H5 and H2-H4 become even more antibonding (overlap population of −0.092 e⁻, cf. Table V). If one such pair, say H1-H5, is brought together to form the product hydrogen molecule, the pairwise interaction becomes even more repulsive (overlap population of −0.313 e⁻; C_{2v}*, Table V) before the requisite HOMO-LUMO inversion occurs on the way to products. In the LMO picture, a H1-B-H5 three-center orbital is formed (C_{2v}*, Table IV), but H1 and H5 have opposite phases prior to the HOMO-LUMO inversion, and a high activation barrier[34] results. A pair which consists of one basal and one axial hydrogen has a slightly negative overlap population in the C_{4v} structure (−0.026 e⁻) and the elimination of such a pair as H_2 has a PRDDO energy barrier of ~11 kcal/mol.

Similarly, both the LMO results and the overlap populations establish H1-H4 and H4-H5 as the favored pairs for elimination as hydrogen from the C_{2v} structure (Figure 5). Again, these pairs in the C_{2v} structure correspond in the D_{3h} structure to equatorial-axial interactions which have been enhanced as a result of the geometrical deformation. One of these three-center bonds (e.g., H4-B-H5) is preserved in the subsequent deformation to C_s symmetry (cf. Figure 3d), making possible a smooth conversion to BH_3 and H_2. Other pairs, such as H3-H5, represent concomitantly weakened axial-equatorial interactions; the modest negative overlap population of −0.014 e⁻ for H3-H5 produces a small PRDDO barrier of ~9 kcal/mol for evolution of hydrogen.

Finally, we note that the LMO's of the C_{4v} structure go smoothly over into those of the lower energy configuration of C_{2v} symmetry (Figure 5). Hence, this transformation (Figure 3c) can proceed spontaneously, as reported above. In each case, the LMO results and the overlap populations conveniently indicate those hydrogen motions which can result in a smooth conversion of the MO's of BH_5 to those of BH_3 and H_2, as well as those which must induce or enhance energetically unfavorable interactions.

Intramolecular Rearrangement in BH_5

As noted above, the fact that most of the hydrogen evolved from BH_4^- in D_2O or BD_4^- in H_2O is HD[2-4,6] strongly implies that the incoming proton or deuteron largely adopts and maintains a position in the "H_2" subunit. If, instead, the entering proton (or deuteron) had occupied one of a set of three or more equivalent positions, a substantial fraction of D_2 would have been evolved in the reaction of BD_4^- in H_2O. Thus, Mesmer and Jolly report a composition of 3.1% H_2, 95.6% HD, and just 1.3% D_2 from complete hydrolysis of BD_4^- in H_2O at room temperature;[3] the 3% H_2 is principally a measure of the extent of exchange with solvent prior to hydrolysis. Similarly, the hydrolysis of BH_4^- in D_2O yields ~4% D_2.[3] While a secondary intermediate having three or more equivalent hydrogen-loss positions might play a minor role, we shall take

the above as evidence for a slow, but detectable, internal rearrangement (scrambling) in BH_5.

In order to examine the facility of internal rearrangement, we constructed optimized *quadratic synchronous transit* (QST) pathways[32] [Figures 6a–c] for three prospective internal rearrangement processes of the C_s(I) (upper curves) and C_s(III) structures for BH_5. In each case, two or more hydrogens are permuted among the unique C_s symmetry positions. QST's are three-point interpolation pathways[32] which here are based on PRDDO optimized initial, intermediate, and final structures (solid symbols). The intermediate structures were first generated via linear synchronous transits[31] and were then fully optimized energetically at constant *path coordinate, p* (*orthogonal optimization*).[32]

In Figure 6a we show the optimized QST's for the following double interchange:

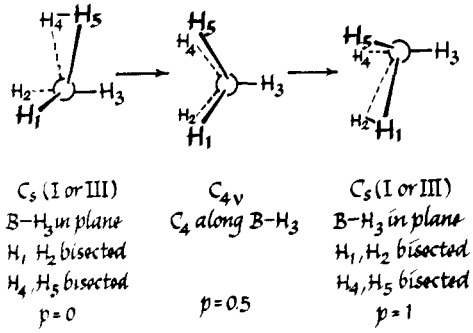

(1)

C_s (I or III) — B–H_3 in plane; H_1, H_2 bisected; H_4, H_5 bisected; $p = 0$

C_{4v} — C_4 along B–H_3; $p = 0.5$

C_s (I or III) — B–H_3 in plane; H_1, H_2 bisected; H_4, H_5 bisected; $p = 1$

For both the C_s(I) and C_s(III) processes, the optimal half-way point (p = 0.5) was found to be just the C_{4v} structure previously characterized. For this process, the computed PRDDO barrier to rearrangement is 34 kcal/mol for the C_s(III) structure, but is just 5 kcal/mol for the higher energy C_s(I). Using the PRDDO structures, we found the two barriers to be 32 and 15 kcal/mol, respectively, when evaluated at the 4-31G level. The analogous exchange of H4–H5 with H1–H3 (or H2–H3) was not examined, but would be expected to yield an essentially identical barrier, because H4–H5 can rotate nearly freely above the BH_3 subunit.

We next considered the process shown in equation 2. Here,

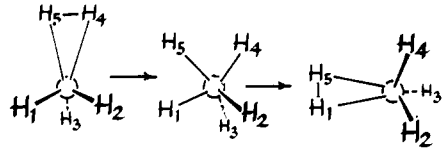

(2)

C_s — B–H_3 in plane; H_4H_5 bisected; H_1H_2 bisected; $p = 0$

C_s — $BH_5H_2H_3$ in plane; $p = 0.5$

C_s — B–H_3 in plane; H_1H_5 bisected; H_2H_4 bisected; $p = 1$

H1 and H4 interchange identities and become equivalent at the midpoint of the path. The midpoint structure displays C_s symmetry and has a mirror plane which passes through B, H2, H3, and H5. The barrier to rearrangement of the C_s(III) structure is 24 kcal/mol when computed at the PRDDO level (Figure 6b) and 19 kcal/mol when evaluated via 4-31G calculations. The pair of C_s(I) structures, however, can interconvert without activation at the PRDDO level, and encounter a barrier of only 4 kcal/mol at the 4-31G level.

Third, we examine in Figure 6c a process (eq 3) which interchanges H1 with H4. Apart from the labeling of the atoms, the optimized midpoint structure in this case is in fact identical with that obtained for process 2, and hence the respective PRDDO and 4-31G barriers are also the same. Equivalent barrier heights should have been expected because H4–H5 is

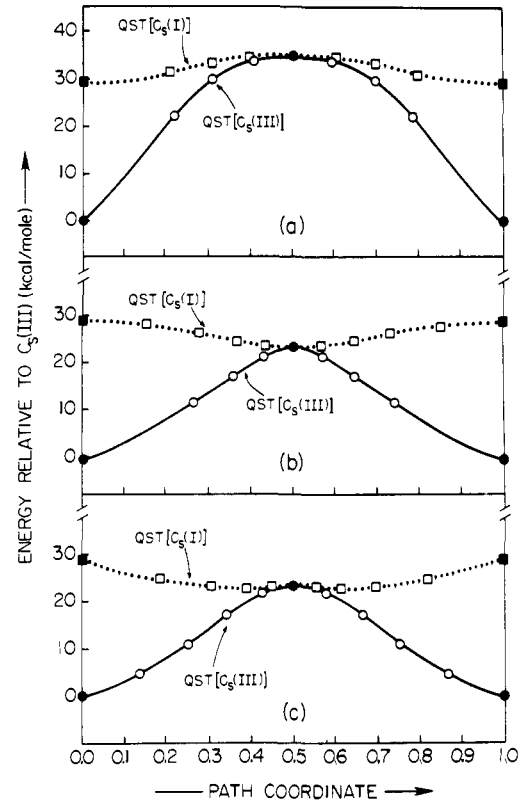

Figure 6. Optimized quadratic synchronous transit pathways for interconversions of C_s structures for BH_5 [eq 1–3]. Solid symbols represent structures optimized at constant path coordinate.

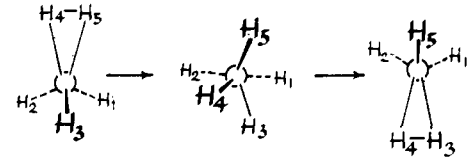

(3)

C_s — B–H_3 in plane; H_1H_2 bisected; H_4H_5 bisected; $p = 0$

C_s — $BH_1H_2H_4$ in plane; $p = 0.5$

C_s — B–H_5 in plane; H_1H_2 bisected; H_4H_3 bisected; $p = 1$

essentially free to rotate above the BH_3 subunit, as noted above.

Finally, we have considered a process which differs from (3) only in that H4 passes across the face in such a way as to take up the *right-most* position in the H_2 subunit. Here, B, H3, H4, and H5 all lie in a common plane at the midpoint of the pathway, and the symmetry is C_{2v}; this structure, which marks the top of the barrier, lies less than 0.3 kcal/mol above the C_s midpoint for (3) in the PRDDO calculations, but is about 0.6 kcal/mol lower when evaluated at the 4-31G level.

For the most part, the symmetries reported above for the midpoint structures were not assumed in advance, but were derived from the calculations themselves. We note that the specific PRDDO and 4-31G barrier heights obtained here can serve as only qualitative guides, in view of the limits in the applicability of these methods to BH_5 (see later). Even so, a useful result does emerge from these studies of pathways; the previously characterized C_{2v} and C_{4v} structures essentially represent optimal *transition states* for interconversions of the C_s structures. Other rearrangement processes are conceivable, but none of these seemed to us to be particularly attractive candidates. Qualitatively, these results show that internal re-

Table VI. Mulliken Atomic Populations, q

	CH_5^+	CH_5^{+a}	CH_3^+	BH_5 C_s(II)	BH_5 C_s(III)	BH_3	H_2
$q(H_1)$	0.80	0.79	0.74	1.10	1.12	1.11	
$q(H_{4,5})$	0.73	0.75		0.88	0.91		1.0
q(B, C)	6.14	6.13	5.77	4.96	4.86	4.68	

[a] CH_5^+ for which distal hydrogens $H_{4,5}$ have exponents of 1.20.

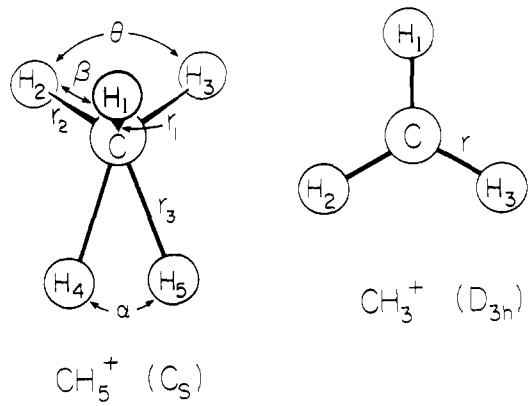

Figure 7. Optimized structures for CH_5^+ ($r_1 = r_2 = 2.032$ au, $r_3 = 2.535$ au, $\theta = 113.4°$, $\alpha = 39.2°$, $\beta = 113.4°$) and CH_3^+ ($r = 2.045$ au).

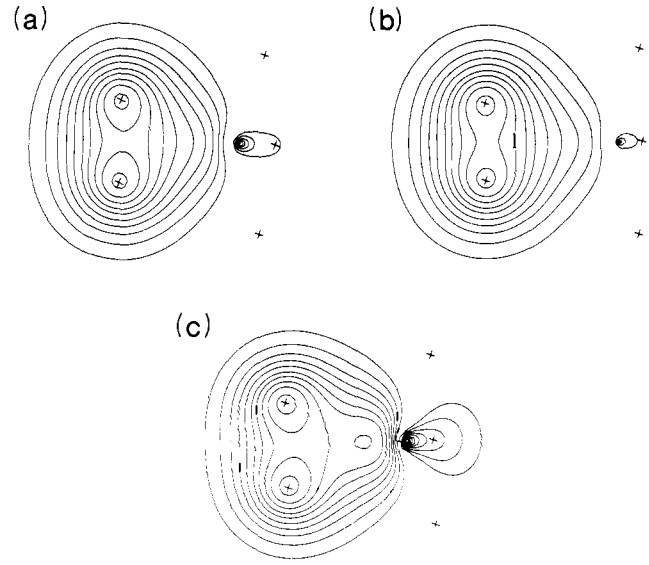

Figure 8. Electron density (PRDDO) for the three-center H-B(C)-H′ localized orbitals in (a) the C_s(II) and (b) the C_s(III) structures for BH_5, and (c) CH_5^+(C_s) in the H-B(C)-H′ plane. Contour levels shown (e/au^3) are 0.25, 0.17, 0.13, 0.1, 0.08, 0.06, 0.045, 0.032, 0.02, and 0.01 in each case. Crosses mark the atomic positions.

arrangement in BH_5 is not inordinately difficult but should not occur extensively unless BH_5 is formed from $BH_4^- + H^+$ with considerable excess internal energy.

Comparison of BH_5 and CH_5^+. We now consider in detail possible reasons for the apparent difference in relative stability of BH_5 and CH_5^+. Intuitively, one would expect CH_3^+ to bond molecular hydrogen more tightly than does BH_3, simply because of the former's positive charge. In order to compare actual charge distributions and bonding descriptions, we optimized structures for CH_5^+ and CH_3^+ (Figure 7) with PRDDO, and localized the PRDDO wave functions for CH_5^+, CH_3^+, BH_5, and BH_3[35] using the Boys criterion[26,27] (Table IV). For comparison with CH_5^+ we selected a structure along the computed C_s pathway for BH_5 whose distal B-H and H-H distances differed negligibly from those of CH_5^+.[36] As shown in Table III, this structure [C_s(II)] is lower in energy than the D_{3h}, C_{4v}, C_{2v}, or initial C_s(I) configurations. The results of localizing the MO's for C_s(II) are presented in Table IV, and the overlap and atomic populations are given in Tables V and VI. For comparison, we have also included the results for the C_s(III) structure in which the distal C-H and B-H distances are matched proportionately, rather than absolutely. For both comparable and proportional H4-H5 distances, we find that the PRDDO overlap population for the atom pair H4-H5 is significantly larger in BH_5 [0.56 e$^-$, C_s(II); 0.68 e$^-$, C_s(III)] than in CH_5^+ [0.41 e$^-$], and that the B-H4 and B-H5 overlap populations [0.20 e$^-$, C_s(II); 0.11 e$^-$, C_s(III)] are somewhat smaller than their C-H counterparts [0.27 e$^-$]. In the localized molecular orbital framework, most of the interactions involving H4 and H5 are partitioned into the three-center H4-B(C)-H5 bond of the pentacoordinated species (Table IV). Here we also find greater electron populations on H4 and H5 in BH_5 [0.86 e$^-$, C_s(II); 0.91 e$^-$, C_s(III)] than in CH_5^+ [0.72 e$^-$], and a correspondingly smaller population on boron [0.32 e$^-$, C_s(II); 0.21 e$^-$, C_s(III)] than on carbon [0.58 e$^-$]. Indeed, the total Mulliken populations on H4 and H5 in CH_5^+ show that ~0.5 electron is transferred from H_2 to the CH_3^+ subunit, as compared to a transfer of only about 0.2 electron in BH_5 (Table VI). These differences are strikingly evident in the electron density maps for the three-center LMO's (Figure 8) and fully confirm the intuitive expectation that the positively charged CH_3^+ should more readily bond H_2 than should BH_3.

As a check on the sensitivity of these results to the choice of exponent, we substituted hydrogen-molecule exponents (1.20) for the ab initio optimized distal hydrogen exponents in CH_5^+ (1.29).[14] Although Mulliken charge distributions sometimes depend significantly on the choice of exponent,[21] we found that here the choice of exponent was not a significant factor (Table VI).[37]

Dissociation of BH_5 to BH_3 and H_2

As noted above, the PRDDO method indicated that BH_5 is less stable than BH_3 and H_2 by some 28 kcal for the C_s(III) structure, and 56 kcal for the C_s(I) structure (Table III). In this section we consider the effect of using STO-3G and 4-31G basis sets at the SCF level, estimate the effects of configuration interaction, investigate some solvation effects, and finally consider the relationship of these calculations to the experimental results of others as outlined in the introduction of this paper.

As shown in Figure 4, minimum basis set STO-3G and extended basis set 4-31G calculations[29] on PRDDO optimized C_s structures for BH_5 again yielded smooth, monotonic dissociation curves. The exothermicity for dissociation decreased somewhat as the sophistication of our computational methods increased, but even refinement at the 4-31G level of the angle α (cf. Figure 2d) left the C_s structures several kcal/mol above separated $BH_3 + H_2$.[38]

The C_s(III) structure, which is rather like the optimized CH_5^+ structure,[15,16] contains distal B-H lengths of 2.8 au, which are larger than the distal C-H lengths of 2.5 au[15,16] by the ratio of usual B-H (2.25 au) and C-H (2.06 au) lengths for single bonds. Use of the extended basis set of Laws, Stevens, and Lipscomb[21] (double zeta plus polarization) for BH_3 and

the C_s(III) structure for BH_5, and the optimal (1s, 2s, 2p) basis set for H_2 of Fraga and Ransil,[39] gave essentially the same result as the 4-31G calculation, i.e., a C_s(III) structure ~12 kcal/mol above the separated $BH_3 + H_2$.[38,40] A similar extension had previously stabilized CH_5^+ relative to CH_3^+ and H_2[18,19] by an additional ~6–9 kcal/mol. Complete optimization of parameters other than the distal B–H length might further stabilize BH_5, but our conclusion is that BH_5 is not predicted to be stable toward dissociation to BH_3 and H_2 at the Hartree–Fock limit.

An estimate of electron correlation suggests only marginal stability at best for BH_5. CH_5^+ was further stabilized with respect to $CH_3^+ + H_2$ by ~21 kcal/mol by the inclusion of configuration interaction (CI) at the extended basis set level;[18] however, BH_5 is less compact than CH_5^+, and is therefore likely to show much less stabilization. In fact, the C_s(III) structure of BH_5 is stabilized by only ~2 kcal/mol relative to $BH_3 + H_2$ (Figure 4) in a minimum basis[41] set PRDDO-CI calculation in which all single and double excitations were included;[31] the same calculation gave 5–6 kcal of stabilization for CH_5^+. Of course, no direct comparison can be made of CI stabilizations when different basis sets are used, but it appears likely that CI would not stabilize the C_s(III) structure by more than 7–10 kcal if an extended basis were used. An additional 1–2 kcal/mol stabilization for BH_5 relative to $BH_3 + H_2$ must be included for the quadruple excitations which correspond to simultaneous double excitations in BH_3 and H_2.[42,43] A similar situation arises in the dissociation of B_2H_6, where single and double excitations stabilize $2BH_3$ at large separation by 2 kcal less than twice the CI stabilization of BH_3.[20] Our conclusion here is that the probable CI stabilization of 8–12 kcal/mol of C_s(III) BH_5 would approximately balance the instability at the SCF level, and that this balance is not strongly dependent on the distal B–H lengths.[38] If we have underestimated either the CI stabilization, or if further optimization yields a slight additional stability for BH_5, then BH_5 would be stable in the gas phase.[44]

Solvation effects were studied first in specific hydration models, and then in cavity or continuum models. The interaction[45] of BH_3 at an initial distance of 6 au from H_2O (lone pair donor, Figure 9a) was completely optimized (Figure 9b) at the PRDDO level to an energy of ~60 kcal/mol below that of separated BH_3 and H_2O. Addition of a second H_2O (Figure 9c) did not significantly change the geometry or energy, and yielded the same result as an optimization starting from two H_2O's equidistant from BH_3 (Figure 9d). At the STO-3G and 4-31G levels, partial reoptimizations placed the BH_3:H_2O stabilizations at 49 and 15 kcal/mol, respectively.[38] A value of 5.5 kcal/mol for stabilization of BH_3:H_2O (STO-3G coordinates) was found earlier[46a] at the 6-31G* level. Thus we see here a trend toward decreasing stabilization as the basis set is improved. A similar sensitivity to the choice of basis set also has been reported for BH_3:NH_3.[46] Now, we use a statistical method due to Birge et al.[47] to examine the energy of solvation, E_{solv}, of the BH_3:H_2O complex, where E_{solv} consists of E_{vdW} (the van der Waals interaction between the complex and nearest neighbor solvent molecules), E_{es} (the static and induced solvent-solute dipole-dipole interactions), and E_{cav} (the energy of creation of a cavity); this method neglects specific hydrogen bonding. We find that the BH_3:H_2O complex is destabilized by ~0.5 kcal/mol (Table VII). Combining this information with earlier results, including an estimate for geometry optimization, we find the solvation energy of BH_3 at the 6-31G* level to be roughly 6–8 kcal/mol.

Now, for BH_5 we employ the statistical method directly. Using the 4-31G dipole moment of 1.92 D for the C_s(III) structure, we find a destabilizing solvation energy[48] of about +1 kcal/mol. However, this result is proportional to the square of the dipole moment; a value of 2.5 D would give an electrostatic energy of −16.3 kcal/mol, and hence a solvation energy of −6.2 kcal/mol. In view of these difficulties, we also examined a specific $H_2O \cdots BH_3^{\delta-} \cdots H_2^{\delta+} \cdots OH_2$ complex based on the C_s(III) BH_5 structure. Optimization at the PRDDO level for fixed distal B–H lengths of 2.81 au gave an O–B (left side) distance of 3.83 au and a B–O (right side) distance of 5.15 au. This PRDDO complex is more stable than separated C_s(III) $BH_5 + 2H_2O$ by 7 kcal. In a 4-31G calculation, the B–O interaction is stabilizing by 2 kcal/mol; however, the O–B interaction is very weakly repulsive. Unless electron correlation enhances these interactions, particularly the latter, we conclude that hydration alters the energy curve very little over the range of distal B–H distances for which a stable BH_5 might reasonably be found. Hence, solvation effects do not appear to aid in stabilizing BH_5 relative to BH_3 and H_2.

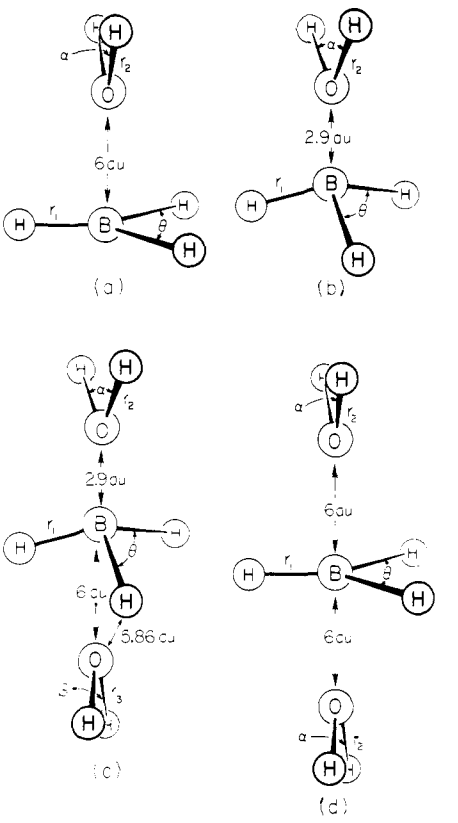

Figure 9. (a) Initial geometry for BH_3:H_2O complex: r_1 = 2.211 au, r_2 = 1.886 au; θ = 120.00°; α = 98.98°. (b) PRDDO optimized BH_3:H_2O complex: r_1 = 2.228 au; r_2 = 1.870 au; θ = 114.16°, α = 110.47°. (c) and (d) Initial geometries for $BH_3(H_2O)_2$ complexes based on (a) and (b). Structural parameters are as defined above.

Table VII. Solvation Energies from the Statistical Interaction Model[a]

$$E_{solvation}{}^{b,c} = E_{vdW} + E_{es} + E_{cav} + E_{or}{}^{d}$$

Parameter	Energies[e]		
	C_s(I)	C_s(III)	BH_3:H_2O
van der Waals (dispersion)[f]	−2.517	−2.737	−4.047
Cavity formation	11.923	12.768	19.160[g]
Electrostatic interaction	−13.876	−9.401	−14.810
Solvation energy	−4.470	0.630	0.303

[a] Cf. ref 47 and 48. [b] Cf. text. [c] The units are kcal/mol. [d] This contribution of E_{or} is negligible in this case, and is therefore omitted. [e] These values are calculated for 4-31G dipole moments. [f] These values are based on 15 nearest neighbors. [g] This calculation employed an elliptical cavity.

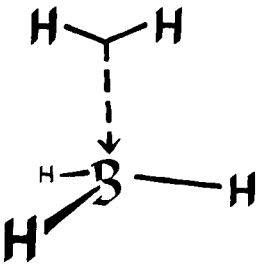

Figure 10. Bonding in BH_5.

We have considered other effects that might stabilize BH_5 and therefore account for its estimated lifetime (see later) of $\sim 10^{-10}$ s in solution. The entrance of H^+ to BH_4^- could produce a force on one of the resident hydrogens away from boron, and thus could generate an asymmetric vibration mode for the relative motion of the new B–H and previously existing, but elongated, B–H bond; conversion to a symmetric mode would then result in loss of H_2. Unfortunately, the time scale for this change of mode is usually $\leq 10^{-12}$ s.[49] Probably, a similar comment applies to the trapping of an excited rotational mode of the BH_5 complex. Hence, a dynamical explanation sems untenable.[50] Next, we considered the possibility that the intrinsic pressure of water (10^{+3} atm) might confine the complex, but the forces seem too small by about two orders of magnitude.[51] Finally, a specific structure effect of water could conceivably confine BH_5; however, both exchange and hydrogen loss are found for hydrolysis of BD_4^- in moist tetrahydrofuran,[52] which is likely to have a different solvent structure effect.

Comments on Experimental Results. In the mechanism (Figure 1) due principally to Kreevoy and Hutchins,[4] protonation of BH_4^- by D_3O^+ dominates up to pH $\simeq$ 12; deprotonation by OD^- becomes competitive, and ultimately suppresses hydrolysis, only above pH 13. At pH 10 exchange (via deprotonation by D_2O) and hydrogen loss occur with relative rates of 1:10.[22,52] The fact that hydrogen is lost as HD implies either that the D^+ added to BH_4^- (a) becomes functionally equivalent to only one resident hydride (e.g., BH_3:HD, in C_s symmetry), or (b) is unique *and* is lost when "hydrogen" is expelled. A candidate for (b) is the C_{4v} structure where D is on the four-fold axis, as suggested by Kreevoy and Hutchins.[4] However, process (b) is incompatible with our molecular orbital studies. Hence, we consider, as did Kreevoy and Hutchins, only C_s symmetry, in particular, the C_s(III) BH_5 structure, within possibility (a).

Kreevoy and Hutchins[4] find that the rate of hydrolysis (hydrogen evolution) is given by $k_1^{Hyd}[BH_4^-]$, where

$$k_1^{Hyd} = [k_{H^+}[H_3O^+] + k_{H_2O}]\left\{\frac{k_{H_2loss}}{k_{H_2loss} + k_{depr}[OH^-]}\right\} \quad (4)$$

The term in the square brackets represents the total rate of protonation of BH_4^-, and the term in curly brackets (the fractionation term) expresses the probability that BH_5 will lose molecular hydrogen rather than be deprotonated by OH^-. Deprotonation by H_2O also occurs,[53] as noted above, but this is a minor perturbation which need not concern us here. At very high pH, the experimental rate of hydrolysis falls rapidly to zero in a way which is consistent with the dependence of the fractionation term on $[OH^-]$. This $[OH^-]$ dependence strongly indicates that exchange with solvent (via deprotonation) and hydrogen loss in fact proceed through a common intermediate, for otherwise the rate of hydrolysis ought to be unaffected, apart from a possible medium effect, by a change in $[OH^-]$ or $[OD^-]$. We accept this as evidence for a common intermediate, which we shall take to be BH_5.

The kinetic analysis[4] further indicates that the fractionation term falls to $\sim$0.5 when $[OH^-]$ reaches $\sim$1 M; then, k_{H_2loss} and $k_{depr}[OH^-]$ are approximately equal. We can therefore infer the intrinic lifetime for BH_5 determined by its rate of hydrogen loss provided that we can reliably estimate the rate for its deprotonation in 1 M OH^-. Since OH^- is a much stronger base than is BH_4^-, the deprotonation of BH_5 by OH^- is expected to be strongly exothermic. Indeed, there is an appreciable activation energy for hydrolysis of $\sim$23 kcal/mol when BH_4^- is protonated by H_2O in the reverse of the process under consideration.[3] The choice of a diffusion controlled value[54] for k_{depr} of $\approx 10^{10}$ M^{-1} s^{-1} then yields $\sim 10^{10}$ s^{-1} for k_{H_2loss}. We therefore take 10^{-10} s as a "lifetime" for BH_5. We suggest that the 10^3 factor over 10^{-13} s (kT/h) indicates some kind of barrier in solution of about 5 kcal/mol; such a treatment would neglect the entropy effects in the transformation of a possibly solvent-stabilized BH_5 to its dissociable transition state.[38] If the deprotonation step has a barrier, i.e., is not diffusion controlled, the lifetime could be longer. Also, if the preexponential factor is like that of 10^{16} s^{-1} for ethane decomposition to methyl radicals, the activation barrier is 8.4 kcal for the rate constant of 10^{10} s^{-1} for BH_5 at 25 °C. Thus, our computational results differ from experiment by some 5–10 kcal/mol, and we suspect that our theoretical models are inadequate to this extent.

Last, we comment on the results obtained by Olah and coworkers[5] upon treatment of excess solid $NaBH_4$ or $LiAlH_4$ with anhydrous D_2SO_4 or DF (or isotopic inverses) in a bomb at −78 °C. Typically $\sim$60% H_2 and 40% HD (plus 2% D_2) is found. These values are essentially statistical if we assume that the gaseous BH_3 or BH_2D evolved escape further reaction with acid. Here, the reaction may possibly occur on the crystal surface in such a way as to physically confine the BH_4D sufficiently to promote internal rearrangement. More likely, these results may simply be due to the different solvent system. That is, the BH_4D system may be formed at an internal energy higher than possible in an aqueous system, owing to the strongly acid nature of anhydrous D_2SO_4 and DF, and this excess internal energy may allow BH_4D to rearrange readily. Further study of this heterogeneous system is needed in order to clarify the possible reasons for these different results.

Added Comments. New results on BH_5, BH_3, and H_2 allow us to assess the contributions of polarization functions to the stabilization of BH_5. Our SCF and SCF-CI calculations with double ζ basis sets utilized optimized exponents of Roetti and Clementi[55] for boron (1s = 6.5666, 1s′ = 4.2493, 2s = 1.4131, 2s′ = 0.8756, 2p = 2.2173, 2p′ = 1.0055), optimized exponents of Shavitt et al.[56] for H_2 (1s = 1.1220, 1s′ = 1.3860), and exponents for H taken from an optimization of a BH fragment (1s = 1.0197, 2s = 0.9852). The CI calculations included all single and double excitations from valence orbitals to which were added an estimate for the effect of quadruple excitations. Our calculations, when compared with those of Hoheisel and Kutzelnigg[57] and Collins et al.[58] indicate that the bonding between the BH_3 and H_2 subunits is primarily due to the inclusion of polarization functions in the CI calculations. That is, without polarization functions, BH_5 is still some 7 kcal/mol unstable with respect to BH_3 and H_2. Inclusion of polarization functions in the CI may be necessary to describe a stabilizing donor–acceptor behavior in the BH_3 and H_2 subunits.

Finally we add in Figure 10 a simplified description of the bonding in the BH_5 molecule.

Acknowledgment. We wish to thank Professors M. M. Kreevoy and D. R. Herschbach and Dr. R. M. Stevens for helpful discussions and comments, and particularly Dr. R. B. Birge for carrying out the statistical solvation calculations. We wish to thank the Office of Naval Research and the National Institutes of Health Grant GM06920 for support.

References and Notes

(1) Address correspondence to this author.
(2) W. L. Jolly and R. E. Mesmer, Abstracts, 141st National Meeting of the American Chemical Society, Washington, D.C., March 1962, p 4M; W. L. Jolly and R. E. Mesmer, *J. Am. Chem. Soc.*, **83**, 4470 (1961).
(3) R. E. Mesmer and W. L. Jolly, *Inorg. Chem.*, **1**, 608 (1962).
(4) M. M. Kreevoy and J. E. C. Hutchins, *J. Am. Chem. Soc.*, **94**, 6371 (1972).
(5) G. A. Olah, P. W. Westerman, Y. K. Mo, and G. Klopman, *J. Am. Chem. Soc.*, **94**, 7859)1972), and references therein.
(6) R. E. Davis, E. B. Bromels, and C. L. Kibby, *J. Am. Chem. Soc.*, **84**, 885 (1962), and references therein.
(7) G. A. Olah, J. R. De Member, A. Commeyras, and J. L. Bribes, *J. Am. Chem. Soc.*, **93**, 459 (1971), and references therein.
(8) G. A. Olah, *J. Am. Chem. Soc.*, **94**, 808 (1972).
(9) M. D. Sefcik, J. M. S. Henis, and P. P. Gaspar, *J. Chem. Phys.*, **61**, 4321 (1974).
(10) G. A. Olah and R. H. Schlosberg, *J. Am. Chem. Soc.*, **90**, 2726 (1968).
(11) G. A. Olah, G. Klopman, and R. H. Schlosberg, *J. Am. Chem. Soc.*, **91**, 3261 (1969).
(12) W. Th. A. M. Van der Lugt and P. Ros, *Chem. Phys. Lett.*, **4**, 389 (1969).
(13) H. Kollmar and H. O. Smith, *Chem. Phys. Lett.*, **5**, 7 (1970).
(14) J. J. C. Mulder and J. S. Wright, *Chem. Phys. Lett.*, **5**, 445 (1970).
(15) V. Dyczmons, V. Staemmler, and W. Kutzelnigg, *Chem. Phys. Lett.*, **5**, 361 (1970).
(16) W. A. Lathan, W. J. Hehre, and J. A. Pople, *J. Am. Chem. Soc.*, **93**, 808 (1971).
(17) W. A. Lathan, W. J. Hehre, L. A. Curtiss, and J. A. Pople, *J. Am. Chem. Soc.*, **93**, 6377 (1971).
(18) V. Dyczmons and W. Kutzelnigg, *Theor. Chim. Acta*, **33**, 239 (1974).
(19) P. C. Hariharhan, W. A. Lathan, and J. A. Pople, *Chem. Phys. Lett.*, **14**, 385 (1972).
(20) D. A. Dixon, I. M. Pepperberg, and W. N. Lipscomb, *J. Am. Chem. Soc.*, **96**, 1325 (1974), and ref 21.
(21) E. A. Laws, R. M. Stevens, and W. N. Lipscomb, *J. Am. Chem. Soc.*, **94**, 4461 (1972).
(22) M. M. Kreevoy, private communication.
(23) Hydrolysis is so slow that BH_4^- has been recrystallized from extremely basic solutions; cf. V. I. Mikheeva and V. B. Breetis, *Dokl. Akad. Nauk SSSR*, **131**, 1349 (1960).
(24) T. A. Halgren and W. N. Lipscomb, *Proc. Natl. Acad. Sci. U.S.A.*, **69**, 652 (1972); T. A. Halgren and W. N. Lipscomb, *J. Chem. Phys.*, **58**, 1569 (1973).
(25) T. A. Halgren, D. A. Kleier, J. H. Hall, Jr., L. D. Brown, and W. N. Lipscomb, manuscript in preparation.
(26) D. A. Kleier, T. A. Halgren, J. H. Hall, Jr., and W. N. Lipscomb, *J. Chem. Phys.*, **61**, 3905 (1974).
(27) S. F. Boys, *Rev. Mod. Phys.*, **32**, 306 (1960); J. M. Foster and S. F. Boys, *ibid.*, **32**, 300 (1960); S. F. Boys, "Quantum Theory of Atoms, Molecules, and the Solid State", P. O. Löwdin, Ed., Academic Press, New York, N.Y., 1966, p 253.
(28) The density map program was written in this laboratory.
(29) W. J. Hehre, R. F. Stewart, and J. A. Pople, *J. Chem. Phys.*, **51**, 2657 (1969); W. J. Hehre, R. Ditchfield, R. F. Stewart, and J. A. Pople, *ibid.*, **52**, 2769 (1970); R. Ditchfield, W. J. Hehre, and J. A. Pople, *ibid.*, **54**, 724 (1971); W. J. Hehre and W. A. Lathan, *ibid.*, **56**, 5255 (1972).
(30) R. M. Stevens, *J. Chem. Phys.*, **52**, 1397 (1970).
(31) We used programs developed by D. A. Kleier and T. A. Halgren.
(32) T. A. Halgren, I. M. Pepperberg, and W. N. Lipscomb, *J. Am. Chem. Soc.*, **97**, 1248 (1975); T. A. Halgren and W. N. Lipscomb, to be published.
(33) The two three-center bonds can be between any two adjacent hydrogens and the boron; i.e., we actually have a set of symmetry equivalent three-center bonds (appearing as C_{2v} structures in a valence bond picture), because there are not enough localized orbitals to reflect the full C_{4v} symmetry of the wave function.
(34) The initial linear synchronous transit (ref 32) resulted in a barrier of 173 kcal/mol; no optimization was attempted.
(35) For a meaningful comparison, we needed to localize the wave functions of *optimized* PRDDO structures for CH_3^+ and CH_5^+. Beginning with the minimum basis set coordinates of Mulder and Wright (ref 14), we obtained the stable PRDDO structures reported in Table II and Figure 6 for CH_3^+ and CH_5^+. We believe that Mulder and Wright did not completely optimize their CH_5^+ structure; using the same program (i.e., Stevens, ref 30) as they did, we calculated a CH_5^+ energy using our PRDDO optimized coordinates (adjusted for C–H length shortening, cf. ref 20) and found an energy ~5 kcal lower than theirs (−40.318 au). Our structure was comparable to that of Lathan et al. (ref 16 and 17).
(36) The effect of exactly matching H_l and H–H distances (by a configuration not on our pathway) was to change the BH_5 overlap populations, localized orbital populations, and atomic charges on the order of 0.01 e^-.
(37) The effect of substituting the 1.20 exponents was also to change the overlap populations by <0.01 e^-.
(38) Cf. thesis, I. M. Pepperberg, for a more detailed account.
(39) S. Fraga and B. J. Ransil, *J. Chem. Phys.*, **35**, 1967 (1961).
(40) We saw a 2 kcal/mol drop in relative energy when the LSL basis[21] was employed for the H_2 molecule. It therefore appears that the H_2 subunit requires exponents which match that of the H_2 molecule.
(41) Some question has recently arisen as to the use of minimum basis set CI as a means of theoretical analysis. Stevens has found that such a calculation may fail to describe properly the potential curve for a motion which passes through a conformation possessing higher symmetry than that of the initial structure, or one in which there is no 1:1 correspondence between valence and excited state orbital [cf. R. M. Stevens, *J. Chem. Phys.*, **61**, 2086 (1974)]. However, we retain C_s symmetry throughout the CI calculation of BH_5 dissociation, and consequently do not feel that the results of Stevens affect the validity of our conclusions.
(42) R. Ahlrichs, *Theor. Chim. Acta*, **35**, 59 (1974).
(43) E. R. Davidson, "The World of Quantum Chemistry", R. Daudel and B. Pullman, Ed., Rudel Publishing Co., Dordricht, Holland, 1974, p 17; S. R. Langhoff and E. R. Davidson, *Int. J. Quantum Chem.*, **8**, 61 (1974).
(44) We note that Olah and co-workers (cf. ref 5) have proposed the existence of BH_5 as a gas phase intermediate in the reaction of B_2H_6 and D_2.
(45) This intermediate has been observed in methanol–water mixtures; cf. F. T. Wang and W. L. Jolly, *Inorg. Chem.*, **11**, 1933 (1972).
(46) (a) J. D. Dill, P. v. R. Schleyer, and J. A. Pople, *J. Am. Chem. Soc.*, **97**, 3402 (1975); (b) $H_3B{:}NH_3$ only: A. Veillard, B. Levy, R. Daudel, and F. Gallais, *Theor. Chim. Acta*, **8**, 312 (1967), and references therein.
(47) R. B. Birge, M. J. Sullivan, and B. E. Kohler, in press.
(48) R. B. Birge, private communication.
(49) D. R. Herschbach, private communication.
(50) The 4-31G slope of −8 kcal/mol/au at a B–H distal length of 3 au (cf. Figure 4) translates into an outwardly directed force on the H_2 subunits of 6×10^{27} g Å s^{-2}/N_0, where N_0 is Avogadro's number. Assuming an effective mass of 2 g/N_0, the acceleration of 3×10^{27} Å s^{-2} on the H_2 subunit is found to increase the distal B–H distance by 1 Å in $t = 3 \times 10^{-14}$ s. If the slope is 100 times smaller, e.g., −0.08 kcal/mol/au, the time needed becomes $t = 3 \times 10^{-13}$ s.
(51) A pressure of 10^3 atm ≈ 10^8 N/m^2 distributed over a surface area for BH_5 of 20 $Å^2$/molecule corresponds to a total force of ~1.2×10^{26} g Å s^{-2}/N_0 per molecule of BH_5, where N_0 is Avogadro's number. From ref 50, the outwardly directed 4-31G force on the H_2 subunit per mole of BH_5 is ~50 times greater.
(52) R. H. Cornforth, *Tetrahedron*, **26**, 4635 (1970).
(53) W. J. Jolly, private communication.
(54) M. Eigen, *Angew. Chem., Int. Ed. Engl.*, **3**, 1 (1964).
(55) C. Roetti and E. Clementi, *J. Chem. Phys.*, **60**, 4725 (1974).
(56) I. Shavitt, R. M. Stevens, F. L. Minn, and M Karplus, *J. Chem. Phys.*, **48**, 2700 (1968).
(57) C. Hoheisel and W. Kutzelnigg, *J. Am. Chem. Soc.*, **97**, 6970 (1975).
(58) J. B. Collins, P. v. R. Schleyer, J. S. Binkley, J. A. Pople, and L. Radom, *J. Am. Chem. Soc.*, preceding paper in this issue.